Biosensors and Bioelectronics 45 (2013) 129–135

Contents lists available at SciVerse ScienceDirect

Biosensors and Bioelectronics

journal homepage: www.elsevier.com/locate/bios

Mutiscale substrates based on hydrogel-incorporated silicon nanowires for protein patterning and microarray-based immunoassays

Sang Won Han [a], Seulah Lee [b], Juree Hong [b], Eunji Jang [a], Taeyoon Lee [b], Won-Gun Koh [a,*]

[a] Active Polymer Center for Pattern Integration, Department of Chemical and Biomolecular Engineering, Yonsei University, 50 Yonsei-ro, Seodaemun-gu, Seoul 120-749, South Korea

[b] Nanobio Device Laboratory, School of Electrical and Electronic Engineering, Yonsei University, 50 Yonsei-ro, Seodaemun-gu, Seoul 120-749, South Korea

ARTICLE INFO

Article history:
Received 5 November 2012
Received in revised form
11 January 2013
Accepted 30 January 2013
Available online 6 February 2013

Keywords:
Silicon nanowires
PEG hydrogel micropattern
Protein micropatterns
Micropatterned nanostructures
Microarray-based multiplex bioassays

ABSTRACT

Here, protein micropatterns were prepared on micropatterned nanostructures for potential applications in microarray-based multiplex bioassays with enhanced protein-loading capacity and detection sensitivity. Vertically-aligned silicon nanowires (SiNWs) that were about 8 μm in height and 150 nm in diameter were prepared using an etching process and were surface-modified with aminopropyltriethoxysilane (APTES) to allow them to covalently immobilize proteins. The SiNW substrate was then overlaid with a micropattern of poly(ethylene glycol) (PEG) hydrogel to create defined arrays of microwells consisting of APTES-modified SiNW on the bottom of the wells, with hydrogel on the walls of the wells. Due to the non-adhesiveness of PEG hydrogels toward proteins, proteins were selectively immobilized on the surface-modified SiNW regions to create protein micropatterns. The increase in surface area increased the protein loading capacity of the SiNWs by more than 10 times the capacity of a planar silicon substrate. Immunobinding assays between IgG and anti-IgG and between IgM and anti-IgM that were performed on micropatterned SiNWs emitted stronger fluorescent signals and showed higher sensitivity than assays performed on planar silicon substrates. Finally, microfluidic channels were successfully integrated into the micropatterned SiNWs to enable the simultaneous performance of multiple immunoassays on a single microarray platform.

© 2013 Elsevier B.V. All rights reserved.

1. Introduction

Techniques to immobilize proteins in defined patterns on inert matrices enable the study of interactions between different proteins or between proteins and other biomolecules with micro- and nanometer resolution. Applications for such techniques abound in fields such as cell biology, biosensor technology, biomonitoring and tissue engineering (Agheli et al., 2006; Blawas and Reichert, 1998; Jonkheijm et al., 2008; MacBeath and Schreiber, 2000; Valsesia et al., 2008; West, 2011). Most of the protein micropatterning techniques developed in the past decade are either photolithography-based or soft lithography-based, where proteins are immobilized on flat two-dimensional (2D) substrates such as glass, silicon, and gold through non-specific adsorption or covalent binding to a monolayer of functional groups tethered on the surface of the substrate (Cao et al., 2003; Kane et al., 1999; Matsuda and Sugawara, 1995; Novo et al., 2011; Sorribas et al., 2002; Whitesides et al., 2001). However, planar substrates offer limited surface areas for protein attachment and cannot support a biomimetic microenvironment that is compatible with the physicochemical behavior and spatial orientation of various proteins in their native settings. One solution to these problems is to entrap proteins within micropatterned hydrogels (Li et al., 2011; Sung et al., 2009; Yadavalli et al., 2004; Zubtsova et al., 2009). Although the soft and fluidic environment of a fully hydrated hydrogel can provide proteins with near-physiological conditions and can allow the proteins to perform their full range of biological functions, the accessibility of large macromolecules into hydrogel-entrapped proteins is seriously limited due to the highly-crosslinked, small mesh size network within the hydrogels (Lee et al., 2010). Another approach that is used to overcome the disadvantages of planar substrates for protein patterning is to use nanostructures that can offer larger surface areas for protein immobilization and provide more biocompatible environments (Biebricher et al., 2004; Lee et al., 2009, 2012; Rucker et al., 2005; Rusmini et al., 2007). Nanostructures created with dendrimers, fibers, grooves, ridges, pores, wells, and pillars have been protein-immobilized using techniques such as electrospinning, lithography, particle deposition, polymer demixing, and metal evaporation (Ajikumar et al., 2007; Aydin et al., 2009;

* Corresponding author. Tel.: +82 2 2123 5755; fax: +82 2 312 6401.
E-mail address: wongun@yonsei.ac.kr (W.-G. Koh).

0956-5663/$ - see front matter © 2013 Elsevier B.V. All rights reserved.
http://dx.doi.org/10.1016/j.bios.2013.01.062

Chigome and Torto, 2011; Hoff et al., 2004; Kang et al., 2005; Scopelliti et al., 2010; Shin et al., 2002; Son et al., 2010, 2011; Tan et al., 2008; Tsougeni et al., 2010; von der Mark et al., 2010; Wang et al., 2006; Yang et al., 2009; Zhang, 2006). Recently, vertically-aligned nanostructures for immobilizing proteins have received great attention as potential biosensor platforms because they can achieve higher sensitivity and selectivity than planar substrates due to their large surface areas (Anandan et al., 2006). In particular, vertically-aligned silicon nanowires (SiNWs) have attracted wide attention because of their biocompatibility, vast surface-to-bulk ratio, fast response, good reversibility, and ease of surface modification (Yan et al., 2010). However, despite several successful biological uses of vertically-aligned SiNWs such as cell culture and drug delivery (Brammer et al., 2009; Kim et al., 2007; Qi et al., 2009; Shalek et al., 2010), only a few studies describe the construction of vertically-aligned SiNWs with well-defined micropatterns and their subsequent use in protein micropatterning (Piret et al., 2008, 2011). Furthermore, the integration of protein micropatterns on vertically-aligned SiNWs into microfluidic devices for immunoassays has not yet been reported, to the best of our knowledge.

In this study, we fabricated multiscale substrates based on micropatterned nanostructures by overlaying SiNWs with patterned PEG hydrogels, and then we utilized these substrates for protein patterning. The incorporation of PEG hydrogel micropatterns into the SiNWs generated microwells with bottoms composed of numerous SiNWs and walls made of hydrogel, thus creating nanostructures (SiNWs) within the micropatterns (hydrogel). The surfaces of the SiNWs were modified to covalently immobilize protein, and the hydrogel micropatterns were formed high enough to completely encapsulate the SiNWs. Because proteins do not adhere to PEG hydrogels, the proteins were selectively immobilized onto the surface-modified SiNW microdomains, resulting in the creation of protein micropatterns on the micropatterned nanostructures. After confirming that the SiNWs accommodated a higher protein density than planar silicon substrates, we tested the micropatterned SiNWs in microarray-based immunoassay applications.

2. Material and methods

2.1. Materials

Poly(ethylene glycol) diacrylate (PEG-DA) (MW 575), 2-hydroxy-2-methylpropiophenone (HOMPP) (photoinitiator), 3-aminopropyltriethoxysilane (APTES), bovine serum albumin(BSA), BSA conjugated with fluorescein isocyanate (FITC-BSA), and serum from human male AB plasma were purchased from Sigma-Aldrich (Milwaukee, WI, USA). Mouse IgG, mouse IgM, FITC-rabbit anti-mouse IgG (FITC-anti IgG) and Cy3-goat anti-mouse IgM (Cy3-anti IgM) were purchased from ZYMED Laboratories (San Francisco, CA, USA). Glutaraldehyde (2.5% in solution) was purchased from Junsei Chemical (Tokyo, Japan). A micro-BCA protein assay kit was obtained from Pierce (Rockford, IL, USA). Phosphate buffered saline (PBS, 0.1 M, pH 7.4) solutions were purchased from Invitrogen (Carlsbad, CA, USA). The Dow Corning Sylgard 184 poly(dimethylsiloxane) (PDMS) elastomer was purchased from Dow Corning (Midland, MI, USA). The photomasks for photolithography were prepared using AUTO CAD and were printed on transparencies using a standard laser jet printer (LaserWriter 16/600 PS, Apple Inc., Cupertino, CA, USA).

2.2. Instruments

Photo-polymerization of PEG-DA was performed using a 365 nm, 300 mW/cm^2 UV light source (EFOS Ultracure 100ss Plus, UV spot lamp, Mississauga, Ontario, Canada). Protein immobilization onto the silicon substrates was monitored using X-ray photoelectron spectroscopy (XPS) (Kratos Analytical Inc., Chestnut Ridge, NY, USA), and solution absorbance was measured using a VersaMax tunable microplate reader (Molecular Devices, Sunnyvale, CA, USA). Scanning electron microscopy (SEM) was performed using a JEOL T330A at 15 kV (JEOL, Ltd., Tokyo, Japan) to observe substrate morphology. A Zeiss Axiovert 200 microscope equipped with an integrated color CCD camera (Carl Zeiss Inc., Thornwood, NY, USA) was used to obtain the optical and fluorescence images. Fluorescence images were obtained by 568-nm excitation/red emission filter (dichroic mirror 488/568/647; band pass 575–660) for Cy3 and 488-nm excitation/green emission filter (dichroic mirror 488/568/647; band pass 500–560) for FITC, respectively. Image analysis was performed using commercially available image analysis software (KS 300, Carl Zeiss Inc.).

2.3. Fabrication of silicon nanowires (SiNWs)

Vertically-aligned SiNWs arrays were fabricated using the aqueous electroless etching (AEE) method described in our previous work (Seo et al., 2011a). Eight-inch single-polished p-type (100) oriented silicon wafers (8–12 $\Omega\,cm^{-1}$ and the thickness of $\sim$0.725 nm) were fabricated into a planar p–n+ junction wafer via the implantation of phosphorous ion (P+) (dose of 4×1015 ions/cm^2 at an acceleration voltage of 80 keV) and were subjected to a process of activation at 1000 °C for 90 min. The estimated thickness of the n+ doped layer was approximately 1 μm (sheet resistance, Rs = 19 Ω/□). The p–n+ junction wafer was cleaned via successive 5 min ultrasonications in acetone, ethanol, and deionized (DI) water. The etching process on the patterned p–n+ junction Si wafer for fabrication of the selectively grown p–n+ SiNWs was carried out in a solution of hydrofluoric acid (HF) (4.9 M) and $AgNO_3$ (0.03 M) at 60 °C for 60 min. To remove the residual silver nanoparticles and byproducts generated during etching, the sample was immersed in HNO_3 solution for 1 min, followed by careful rinsing with DI water and drying at room temperature.

2.4. Protein immobilization onto the SiNWs

SiNW substrates were immersed in "piranha solution" (a 3:1 mixture of 30% (wt/wt) aqueous sulfuric acid and hydrogen peroxide) for 30 min at 100 °C, washed thoroughly with DI water, and dried under nitrogen. After drying, the substrates were immersed in a solution of 3% (v/v) APTES in 95% (v/v) ethanol under a nitrogen environment for 2 h at room temperature. The substrates were then flushed with ethanol to remove non-covalently bound APTES, and were cured at 115 °C for 2 h. After the APTES treatment, the substrates were immersed in a 2.5% (v/v) solution of glutaraldehyde in PBS for 2 h at room temperature to activate the amine groups in the APTES. After rinsing with deionized water, and drying under nitrogen, the SiNWs were incubated with different protein solutions in PBS (100 μg/mL BSA, or 25.0 μg/mL mouse IgG, or 25.0 μg/mL mouse IgM) for 2 h at room temperature. After reacting with a specified amount of protein, the substrate was removed from the protein solution and the amount of protein that remained in the solution was determined using a micro-BCA protein assay. The difference between the initial and final amounts of protein in solution was defined as the total amount of protein that was immobilized onto the substrate. The surface density of the protein was obtained by dividing the amount of immobilized BSA by the apparent surface area of the substrate. Here, average and standard deviation of five samples ($n=5$) were used to represent each data.

2.5. Fabrication of PEG hydrogel micropatterns on SiNW substrates

PEG hydrogel micropatterns were fabricated from PEG-DA (MW 575) as the base macromer. A precursor solution consisting of 1 mL of PEG-DA and 20 μL of HOMPP was dropped onto the glutaraldehyde-activated SiNW substrates and was then exposed to UV light through a photomask for 2.5 s. Upon UV exposure, the precursor solution underwent free-radical induced gelation and became insoluble in common PEG solvents such as water (Revzin et al., 2001). The desired hydrogel micropatterns were successfully obtained on the SiNW substrates by flushing the substrates with PBS solution. We then incubated the micropatterned substrates with protein solutions for 2 h at room temperature to generate protein micropatterns. The overall procedure for the surface modification of SiNWs with APTES, and for the fabrication of PEG hydrogel micropatterns and protein immobilization were described in Fig. 1a and b.

2.6. Fabrication of the microfluidic system

The microfluidic networks were prepared via replica molding from a 10:1 mixture of the PDMS prepolymer and the curing agent as previously described (Duffy et al., 1998). The resulting mixture was poured onto a silicon master that contained nagative photoresist patterns of microchannels and was cured at 60 °C for at least 5 h. The width of each microchannel was designed to contain two or three columns of SiNW microwells. After curing, the PDMS replica was removed from the master and oxidized in oxygen plasma (Femto Science Inc., Seoul, Korea) for 5 min. The oxidized PDMS microchannels were aligned over the micropatterned SiNWs substrates so that protruding region of the PDMS contacted the PEG hydrogel region and formed the enclosed microchannels as shown in Fig. 1c. The resultant microfluidic device was completed by connecting it to a syringe pump (Harvard Apparatus, Hollistion, MA, USA).

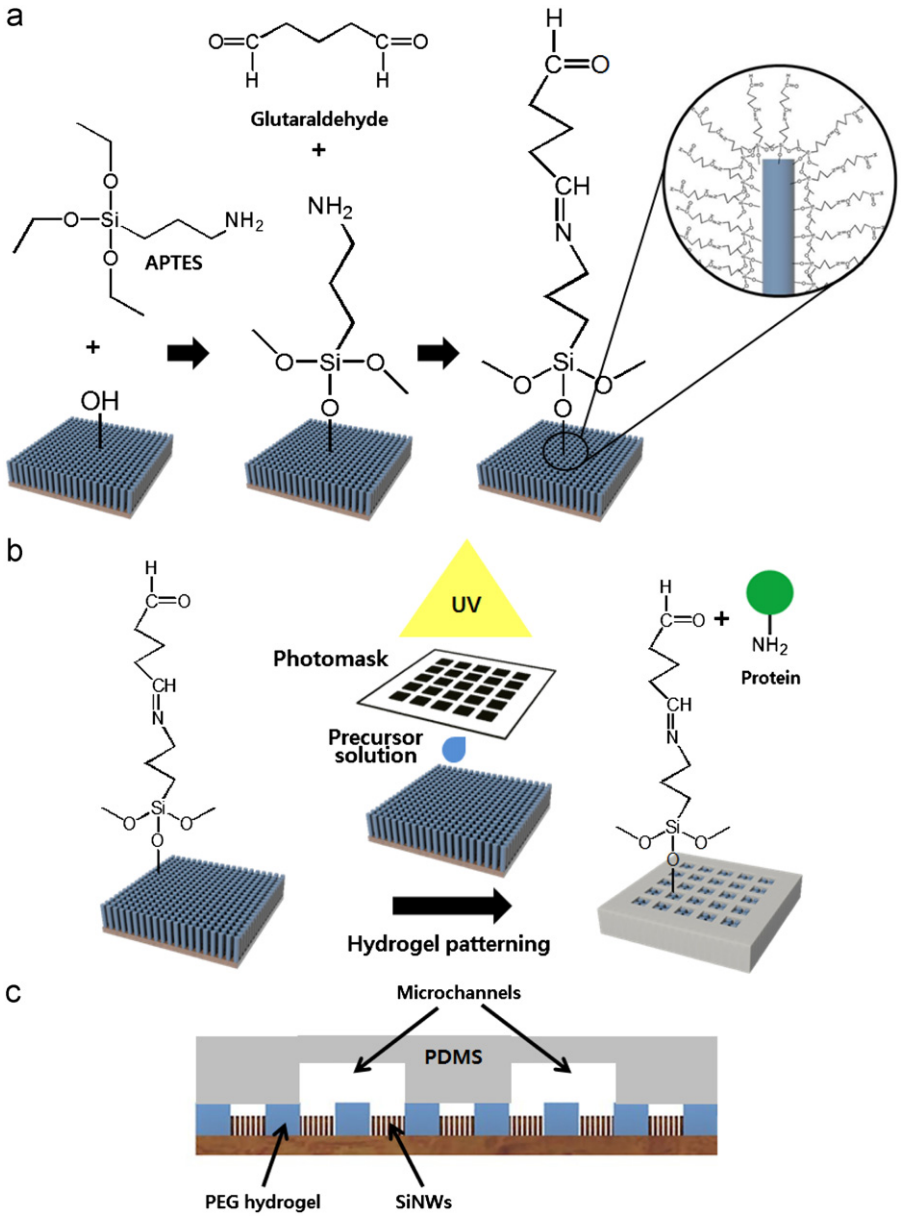

Fig. 1. Schematic illustrations of the preparation of micropatterned SiNWs that covalently immobilized proteins and integration of micropatterned SiNWs with microfluidic channels. (a) The SiNWs were modified with APTES and GA to covalently immobilize proteins. (b) The hydrogel micropatterns were fabricated on surface-modified SiNWs and proteins were immobilized on unpatterned SiNWs. (c) PDMS-based microchannels were integrated with micropatterned SiNWs.

2.7. Immunoassays using micropatterned SiNWs

The SiNW micropatterns were incubated with 25.0 μg/mL mouse IgG or 25.0 μg/mL mouse IgM for 2 h at room temperature. The antibody-activated SiNW micropatterns were then blocked with 1% BSA in PBS for 2 h, and were subsequently reacted with FITC-anti IgG and Cy3-anti IgM at various concentrations for 2 h at 4 °C. The averages and standard deviations of the fluorescence intensities were obtained from three samples ($n=3$), and nine different microdomains ($200\times200\ \mu m^2$) on each sample were quantified as a function of target concentration. For the measurement in serum, different concentrations of Cy3-anti IgM (20–100 ng/mL) were prepared in serum and reacted with immobilized IgM. When the microfluidic system was used, the IgG and IgM solutions were introduced to alternating microchannels that covered different domains of SiNW micropatterns. After covalent immobilization of the IgG and IgM within separate microchannels, the microchannels were flushed with PBS to remove unbound proteins. Solutions containing FITC-anti IgG and/or Cy3-anti IgM were then injected into the microchannels and were allowed to react with the immobilized IgG and IgM. All the reactions within the microchannels were carried out in the stationary state (i.e., we stopped pumping fluids into the device when the microchannels were filled with solution).

3. Results and discussion

As a first step toward the preparation of micropatterned nanostructures, SiNWs arrays were fabricated using the aqueous electroless etching (AEE) method. As shown in Fig. S1, SiNWs of uniform length were successfully fabricated and were aligned vertically over a large area. Fig. S1 further shows that the SiNWs were bundled at their tips by the capillary forces of the liquid during the substrate drying process. The measured diameters and heights of the SiNWs were approximately 150 nm and 8 μm, respectively. The lengths and diameters of the fabricated SiNWs and the densities of the bundled tips were almost identical in all the SiNW samples fabricated under the same conditions.

Proteins were covalently immobilized onto the APTES-modified SiNWs. Silicon surfaces can be easily modified by a silanization reaction with various silane molecules that form a self-assembled monolayer. The surface properties of the silicon substrates can be tailored by changing the functional groups of the silane molecules. Silanization with APTES provided the SiNWs with amine groups as potential protein-immobilization sites. The amine groups in the APTES were converted to aldehyde groups, which reacted with the amine groups in the proteins to form stable imine linkages through activation with glutaraldehyde. The presence of proteins after the immobilization process was confirmed with XPS using BSA as a model protein. As shown in Fig. S2a, the N 1s peak was almost undetectable in the XPS spectrum of a bare SiNW substrate, whereas very high N1s signals were observed in the spectrum of a BSA-immobilized SiNW substrate due to the abundance of peptide linkages. In contrast, the Si 2p peak decreased after immobilization of the BSA, suggesting that the SiNW surface was covered with BSA (Fig. S2b). After confirming that the protein immobilization was successful, the protein-loading capacity of the SiNW substrates was measured via quantification of BSA and was compared to that of flat silicon substrates. Fig. S2c indicates that the SiNW substrates immobilized approximately 14 times more BSA ($57.33\pm4.76\ \mu g/cm^2$) than planar silicon substrates ($4.10\pm4.76\ \mu g/cm^2$). This may be attributed to the increased surface area generated by the high aspect ratio of the SiNWs. Although calculations based on the diameter and height of the SiNWs, as well as on the distance between SiNWs, resulted in a surface area for the SiNW substrate that was 40 times greater than that of the flat silicon substrate, the increase in the actual protein-loading capacity was less attributed to bundling of the SiNWs. A high density of protein immobilized on a binding-specific substrate is shown to enhance the sensitivity and detection limit of a protein-based biosensor. It was therefore expected that a bioassay constructed on a SiNW substrate would show better performance than a similar bioassay performed on a flat silicon substrate.

To prepare micropatterned SiNW substrates, photomasks containing square micropatterns arranged in 50×50 arrays were fabricated. The design of the mask allowed only the hydrogel precursor solution below the transparent region of the photomask to be crosslinked and to become a hydrogel micropattern upon exposure to UV light while residual polymer was removed elsewhere in the pattern. Thus, photopatterning created 2500 SiNWs microwells separated by hydrogel walls that were approximately 25 μm high, as shown in Fig. 2a. A clearly defined array of microwells consisting of SiNW at the bottom and PEG hydrogel walls was successfully fabricated without any residual polymer inside the microwells. The hydrogel micropatterns were high enough to perfectly overlay the SiNWs (10–12 μm) so that no SiNWs occupied the hydrogel region. Therefore, hydrogel patterning created a clear contrast between the protein-repelling PEG hydrogel regions and the glutaraldehyde-activated SiNW regions. The feasibility of selectively immobilizing proteins on the microwells was tested by incubating FITC-BSA with the micropatterned substrates to visualize the localization and patterning of the proteins. Fig. 2b shows fluorescent images of the SiNW microwells incubated with FITC-BSA. The fluorescent and dark regions correspond to the bottom of the SiNW wells with immobilized BSA and the PEG hydrogel walls, respectively. These results indicate that albumin was immobilized only on the SiNW bottoms and that the PEG hydrogel effectively prevented albumin adsorption. Thus, we demonstrated spatial control of protein immobilization on SiNW substrates on a micrometer scale. Furthermore, Fig. 2c shows that the fluorescence intensities were nearly identical from well to well, indicating that uniform amounts of BSA were immobilized within each microwell.

When PEG hydrogel micropatterns are fabricated on flat silicon or glass substrates, those substrate surfaces are usually modified with silane monolayers that have (meth)acrylate end-functional groups that participate in photoinitiated free-radical polymerization to covalently anchor the hydrogel microstructures to the substrates (Revzin et al., 2001). Otherwise, the hydrogel micropatterns easily detach from the surfaces in aqueous environments, as crosslinked hydrogel matrixes swell. Using SiNWs as a substrate for hydrogel micropatterning may prevent the detachment of hydrogel micropatterns, because the precursor solution is able to infiltrate and form crosslinked hydrogel between the SiNWs. That is, the SiNWs act as an adhesion promoter for the hydrogel micropatterns. In the present experiment, detachment of the hydrogel micropatterns was dependent on the height of the SiNW. When the height of the SiNWs exceeded 8 μm, detachment of the hydrogel micropatterns from the SiNW substrates did not occur. Permanent anchoring of the hydrogel micropatterns on the SiNW substrates eliminated the need to use silane adhesion promoters, which in turn allowed us to use other silane molecules such as APTES to immobilize the proteins. This is another important advantage of using SiNWs as substrates, considering that previous studies have used two silane molecules, one to achieve strong adhesion of the hydrogel micropatterns to the substrates and the other for covalent immobilization of proteins (Seo et al., 2011b).

The potential application of the micropatterned SiNWs in biosensing was investigated by constructing two types of immunoassays,

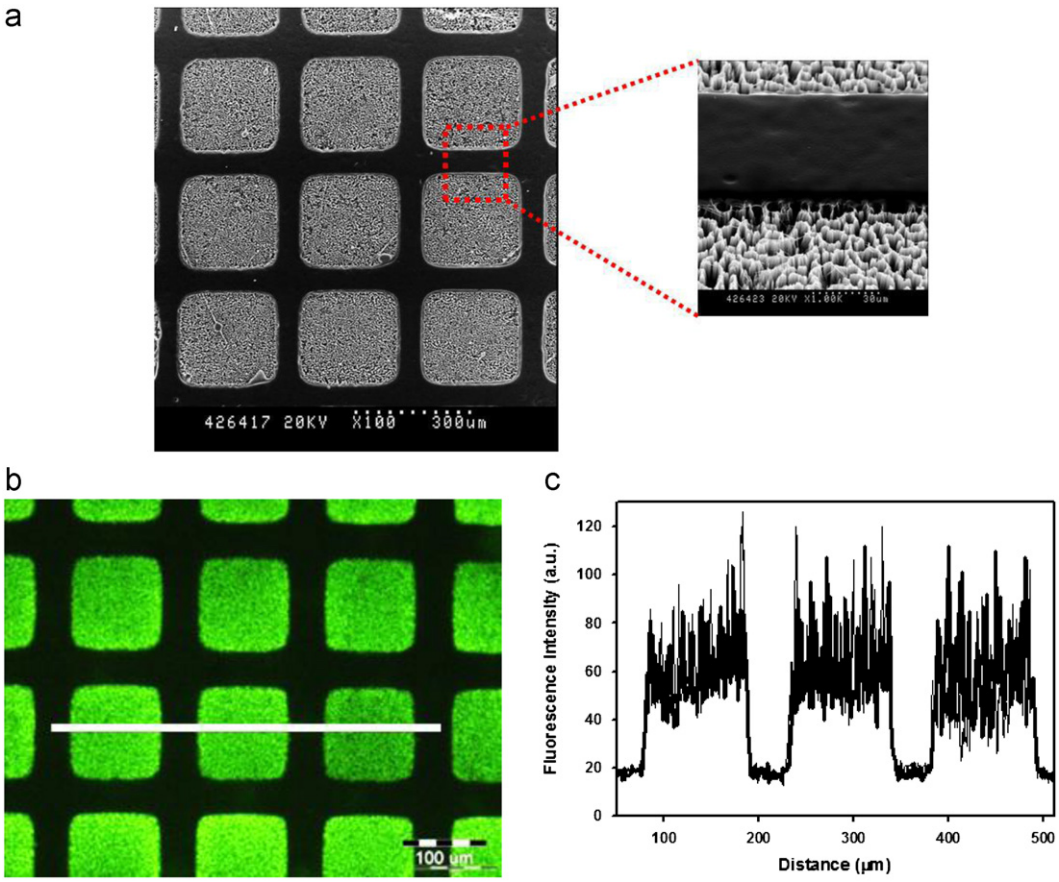

Fig. 2. Fabrication of hydrogel micropatterns onto SiNW substrates and immobilization of FITC-BSA on micropatterned SiNW substrates. (a) SEM images of SiNWs micropatterned with PEG hydrogel. (b) Fluorescent images of a microwell array that was incubated with FITC-BSA. (c) Fluorescence intensity profile across one row of a microwell array that immobilized FITC-BSA.

one using IgG and FITC-anti IgG and the other using IgM and Cy3-anti IgM. Data from the SiNW micropatterns was compared with data from the flat silicon substrates to test the effects of available surface area and corresponding protein-loading capacity on sensing capability. Fluorescent images demonstrated that both the anti-IgG and the anti-IgM bound specifically to the IgG and IgM-immobilized SiNW microdomains, respectively, and that nonspecific adsorption was insignificant in the PEG micropattern regions due to the exclusion effects of the PEG hydrogel against proteins and other small molecules (Fig. 3a and b). Using PEG hydrogel as the background substrate made it possible to skip passivation of the surface, which is necessary for most protein microarray techniques. The immunoassay was quantitatively characterized by measuring the fluorescence intensity of the micropatterns as a function of target concentration. In the binding of both anti-IgG and anti-IgM, fluorescence intensity increased with concentration, and the fluorescence intensity and sensitivity (change in signal per change in concentration) were greatly enhanced using SiNW when compared to flat silicon substrates, as shown in Fig. 3c and d. In regards to the linear range of detection, both anti-IgG and anti-IgM had two different linear range region; 50–100 ng/mL and 100–1000 ng/mL for the anti-IgG and 10–100 ng/mL and 100–1000 ng/mL for the anti-IgM. Under the same conditions, the detection limits of the anti-IgG and anti-IgM were about 1.0×10 ng/mL and 1.0 ng/mL, respectively with SiNW substrates, while the detection limits of both the anti-IgG and the anti-IgM were 1.0×10^3 ng/mL with flat silicon substrates. After demonstrating that our SiNW-based system performed better than the flat silicon substrate-based system, the specificity of our immunoassay system was investigated. For this experiment, different concentrations of anti-IgG and anti-IgM were reacted with immobilized IgM and IgG, respectively. Although fluorescence signals by non-specific binding of both anti-IgM on IgG and anti-IgG on IgM increased with concentration of anti-IgM and anti-IgG as shown in Fig. S3a and b, increase of fluorescence signals by non-specific binding was negligible compared to specific binding shown in Fig. 3c and d. When serum was used instead of PBS solution to investigate the detection performances of the proposed immunoassays in clinical samples, the fluorescence signals were reduced by approximately 10% due to interference by other proteins as shown in Fig. S4.

Finally, PDMS-based microchannels were attached to the micropatterned SiNW substrates to simultaneously carry out multiple immunoassays. In addition to the capability of multiplex assays, the advantages of microfluidic systems over planar-array microchips include enhanced mass and heat transfer, lower sample volumes, and ease of integration with miniaturized sample preparation modules. The simultaneous introduction of IgG and IgM was possible as illustrated in Fig. 4a because the microchannels were isolated from each other and their contents did not intermix. When a solution containing only FITC-anti IgG was injected into all of the microchannels, green fluorescent signals were observed only within the IgG-immobilized microchannels without detectable signals in the IgM-immobilized microchannels due to specific binding between the antibody and the antigen (Fig. 4b), while fluorescent signals were observed only within the microchannels where IgM was immobilized when a solution containing only Cy3-anti IgM was injected (Fig. 4c). In contrast, the introduction of solutions containing both FITC-anti IgG and Cy3-anti IgM resulted in fluorescent signals in all the microchannels as shown in Fig. 4d. These results clearly demonstrated that combining protein micropatterns on

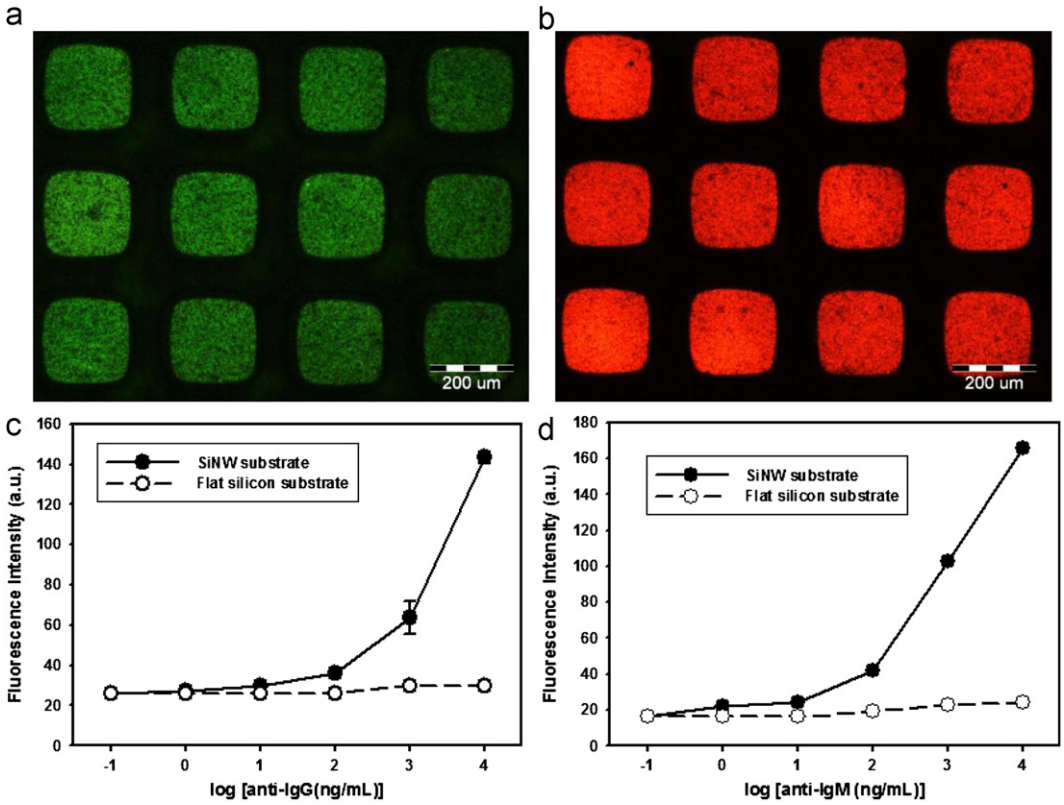

Fig. 3. Immunoassays with micropatterned SiNWs. Fluorescent images obtained from reaction (a) between IgG and FITC-anti IgG and (b) between IgM and Cy3-anti IgM. Change in fluorescence intensity with concentration of (c) FITC-anti IgG and (d) Cy3-anti IgM.

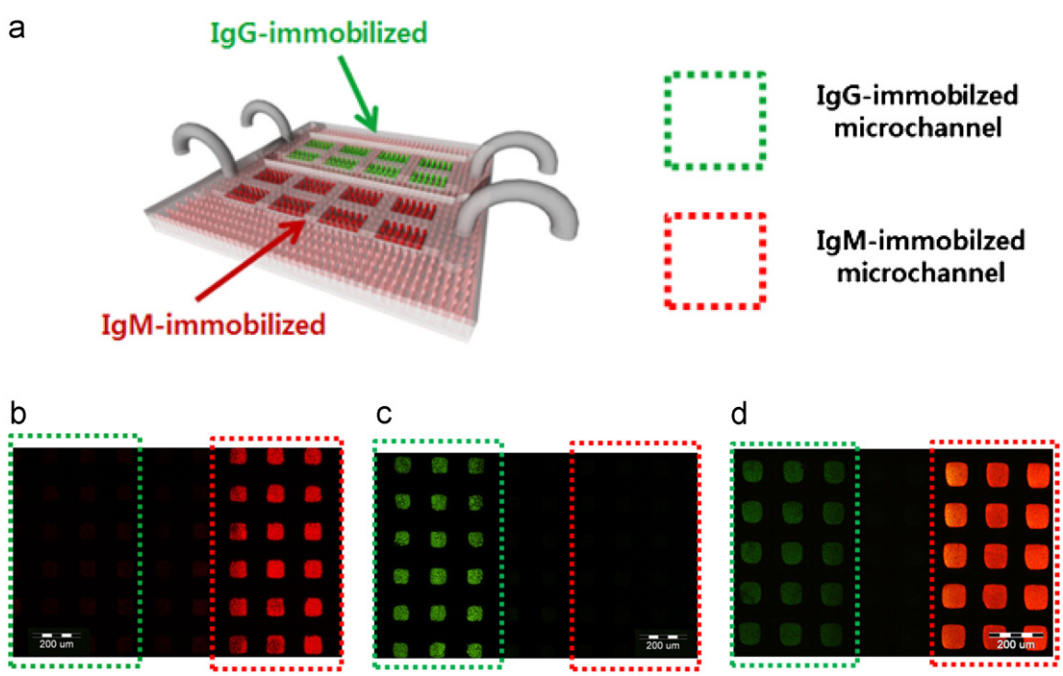

Fig. 4. Integration of PDMS microchannels with micropatterned SiNWs for the simultaneous investigation of multiple immunoassays. (a) Schematic illustration of microchannels contained IgG-immobilized and IgM-immobilized microarray alternatively. Fluorescent images obtained after the microchannels were filled with (b) a solution of FITC-anti IgG only, (c) Cy3-anti IgM only, and (d) a solution containing both FITC-anti IgG and Cy3-anti IgM.

SiNWs with microfluidic channels could create protein microarrays capable of multiplex bioassays with better performance than conventional microarray systems. It should also be noted that our proposed system was perfectly reusable when the SiNWs were cleaned using piranha solution, producing almost same fluorescence intensity upon repeated assays.

4. Conclusion

Protein micropatterns were generated on SiNW substrates for potential applications in highly sensitive protein-based bioassays. The fabrication of PEG hydrogel micropatterns on surface-modified SiNW substrates created arrays of microwells with hydrogel walls and APTES-modified SiNW bottoms. Due to the non-adhesiveness of the PEG hydrogel toward proteins, the target proteins were selectively immobilized on the APTES-modified SiNWs, creating protein micropatterns. In immunoassays based on either IgG and anti-IgG or IgM and anti-IgM specificity, the SiNW micropatterns emitted higher fluorescence intensities and showed higher sensitivities than the corresponding planar substrates, most likely due to the higher protein-loading capacities resulting from the increased surface area. The integration of PDMS microchannels into the SiNW micropattern arrays made the selective immobilization of IgG and IgM onto different domains within a single array platform and the simultaneous detection of both targets possible.

Acknowledgments

This work was supported by the National Research Foundation (NRF) grant funded by the Ministry of Education, Science and Technology (MEST) (2011-0028594, 2012K001321 the "Converging Research Center Program", and R11-2007-050–03002-0 the "Active Polymer Center for Pattern Integration at Yonsei University").

Appendix A. Supporting information

Supplementary data associated with this article can be found in the online version at http://dx.doi.org/10.1016/j.bios.2013.01.062.

References

Agheli, H., Malmstrom, J., Larsson, E.M., Textor, M., Sutherland, D.S., 2006. Nano Letters 6, 1165–1171.
Ajikumar, P.K., Kiat, J., Tang, Y.C., Lee, J.Y., Stephanopoulos, G., Too, H.P., 2007. Langmuir 23, 5670–5677.
Anandan, V., Rao, Y.L., Zhang, G.G., 2006. International Journal of Nanomedicine 1, 73–79.
Aydin, D., Schwieder, M., Louban, I., Knoppe, S., Ulmer, J., Haas, T.L., Walczak, H., Spatz, J.P., 2009. Small 5, 1014–1018.
Biebricher, A., Paul, A., Tinnefeld, P., Golzhauser, A., Sauer, M., 2004. Journal of Biotechnology 112, 97–107.
Blawas, A.S., Reichert, W.M., 1998. Biomaterials 19, 595–609.
Brammer, K.S., Choi, C., Oh, S., Cobb, C.J., Connelly, L.S., Loya, M., Kong, S.D., Jin, S., 2009. Nano Letters 9, 3570–3574.
Cao, T.B., Wei, F., Jiao, X.M., Chen, J.Y., Liao, W., Zhao, X., Cao, W.X., 2003. Langmuir 19, 8127–8129.
Chigome, S., Torto, N., 2011. Analytica Chimica Acta 706, 25–36.
Duffy, D.C., McDonald, J.C., Schueller, O.J.A., Whitesides, G.M., 1998. Analytical Chemistry 70, 4974–4984.
Hoff, J.D., Cheng, L.J., Meyhofer, E., Guo, L.J., Hunt, A.J., 2004. Nano Letters 4, 853–857.
Jonkheijm, P., Weinrich, D., Schroder, H., Niemeyer, C.M., Waldmann, H., 2008. Angewandte Chemie-International Edition 47, 9618–9647.
Kane, R.S., Takayama, S., Ostuni, E., Ingber, D.E., Whitesides, G.M., 1999. Biomaterials 20, 2363–2376.
Kang, M.C., Trofin, L., Mota, M.O., Martin, C.R., 2005. Analytical Chemistry 77, 6243–6249.
Kim, W., Ng, J.K., Kunitake, M.E., Conklin, B.R., Yang, P.D., 2007. Journal of the American Chemical Society 129, 7228–7299.
Lee, A.G., Arena, C.P., Beebe, D.J., Palecek, S.P., 2010. Biomacromolecules 11, 3316–3324.
Lee, Y., Kim, J., Kim, S., Jang, W.D., Park, S., Koh, W.G., 2009. Journal of Materials Chemistry 19, 5643–5647.
Lee, Y., Park, S., Han, S.W., Lim, T.G., Koh, W.G., 2012. Biosensors & Bioelectronics 35, 243–250.
Li, H.Y., Leulmi, R.F., Juncker, D., 2011. Lab on a Chip 11, 528–534.
MacBeath, G., Schreiber, S.L., 2000. Science 289, 1760–1763.
Matsuda, T., Sugawara, T., 1995. Langmuir 11, 2267–2271.
Novo, P., Prazeres, D.M.F., Chu, V., Conde, J.P., 2011. Lab on a Chip 11, 4063–4071.
Piret, G., Coffinier, Y., Roux, C., Melnyk, O., Boukherroub, R., 2008. Langmuir 24, 1670–1672.
Piret, G., Galopin, E., Coffinier, Y., Boukherroub, R., Legrand, D., Slomianny, C., 2011. Soft Matter 7, 8642–8649.
Qi, S.J., Yi, C.Q., Ji, S.L., Fong, C.C., Yang, M.S., 2009. ACS Applied Materials & Interfaces 1, 30–34.
Revzin, A., Russell, R.J., Yadavalli, V.K., Koh, W.G., Deister, C., Hile, D.D., Mellott, M.B., Pishko, M.V., 2001. Langmuir 17, 5440–5447.
Rucker, V.C., Havenstrite, K.L., Simmons, B.A., Sickafoose, S.M., Herr, A.E., Shediac, R., 2005. Langmuir 21, 7621–7625.
Rusmini, F., Zhong, Z.Y., Feijen, J., 2007. Biomacromolecules 8, 1775–1789.
Scopelliti, P.E., Borgonovo, A., Indrieri, M., Giorgetti, L., Bongiorno, G., Carbone, R., Podesta, A., Milani, P., 2010. PLoS One 5, e11682.
Seo, J., Lee, S., Lee, J., Lee, T., 2011a. ACS Applied Materials & Interfaces 3, 4722–4729.
Seo, J.H., Chen, L.J., Verkhoturov, S.V., Schweikert, E.A., Revzin, A., 2011b. Biomaterials 32, 5478–5488.
Shalek, A.K., Robinson, J.T., Karp, E.S., Lee, J.S., Ahn, D.R., Yoon, M.H., Sutton, A., Jorgolli, M., Gertner, R.S., Gujral, T.S., MacBeath, G., Yang, E.G., Park, H., 2010. Proceedings of the National Academy of Sciences of the United States of America 107, 1870–1875.
Shin, K., Leach, K.A., Goldbach, J.T., Kim, D.H., Jho, J.Y., Tuominen, M., Hawker, C.J., Russell, T.P., 2002. Nano Letters 2, 933–936.
Son, K.J., Ahn, S.H., Kim, J.H., Koh, W.G., 2011. ACS Applied Materials & Interfaces 3, 573–581.
Son, K.J., Kim, S., Kim, J.H., Jang, W.D., Lee, Y., Koh, W.G., 2010. Journal of Materials Chemistry 20, 6531–6538.
Sorribas, H., Padeste, C., Tiefenauer, L., 2002. Biomaterials 23, 893–900.
Sung, W.C., Chen, H.H., Makamba, H., Chen, S.H., 2009. Analytical Chemistry 81, 7967–7973.
Tan, Y.H., Liu, M., Nolting, B., Go, J.G., Gervay-Hague, J., Liu, G.Y., 2008. ACS Nano 2, 2374–2384.
Tsougeni, K., Tserepi, A., Constantoudis, V., Gogolides, E., Petrou, P.S., Kakabakos, S.E., 2010. Langmuir 26, 13883–13891.
Valsesia, A., Mannelli, I., Colpo, P., Bretagnol, F., Rossi, F., 2008. Analytical Chemistry 80, 7336–7340.
von der Mark, K., Park, J., Bauer, S., Schmuki, P., 2010. Cell and Tissue Research 339, 131–153.
Wang, C., Zhang, Y., Seng, H.S., Ngo, L.L., 2006. Biosensors & Bioelectronics 21, 1638–1643.
West, J.L., 2011. Nature Materials 10, 727–729.
Whitesides, G.M., Ostuni, E., Takayama, S., Jiang, X., Ingber, D.E., 2001. Annual Review of Biomedical Engineering 3, 335–373.
Yadavalli, V.K., Koh, W.G., Lazur, G.J., Pishko, M.V., 2004. Sensors and Actuators B-Chemical 97, 290–297.
Yan, S.C., He, N.Y., Song, Y.C., Zhang, Z.J., Qian, J.Q., Xiao, Z.D., 2010. Journal of Electroanalytical Chemistry 641, 136–140.
Yang, D.Y., Liu, X., Jin, Y., Zhu, Y., Zeng, D.D., Jiang, X.Y., Ma, H.W., 2009. Biomacromolecules 10, 3335–3340.
Zhang, Y., 2006. Colloids and Surfaces B-Biointerfaces 48, 95–100.
Zubtsova, Z.I., Zubtsov, D.A., Sawateeva, E.N., Stomakhin, A.A., Chechetkin, V.R., Zasedatelev, A.S., Rubina, A.Y., 2009. Journal of Biotechnology 144, 151–159.

[Supplementary Material]

Mutiscale substrates based on hydrogel-incorporated silicon nanowires for protein patterning and microarray-based immunoassays

Sang-Won Han[1], Seulah Lee[2], Juree Hong[2], Eunji Jang[1], Taeyoon Lee[2], and Won-Gun Koh[1, *]

[1] Active Polymer Center for Pattern Integration

Department of Chemical and Biomolecular Engineering, Yonsei University

50 Yonsei-ro, Seodaemun-gu, Seoul 120-749, South Korea

[2] Nanobio Device Laboratory

School of Electrical and Electronic Engineering, Yonsei University

50 Yonsei-ro, Seodaemun-gu, Seoul 120-749, South Korea

*Author to whom correspondence should be addressed. Department of Chemical and Biomolecular Engineering, Yonsei University, 50 Yonsei-ro, Seodaemun-gu, Seoul 120-749, South Korea

E-mail: wongun@yonsei.ac.kr, Phone: 82-2-2123-5755, Fax: 82-2-312-6401

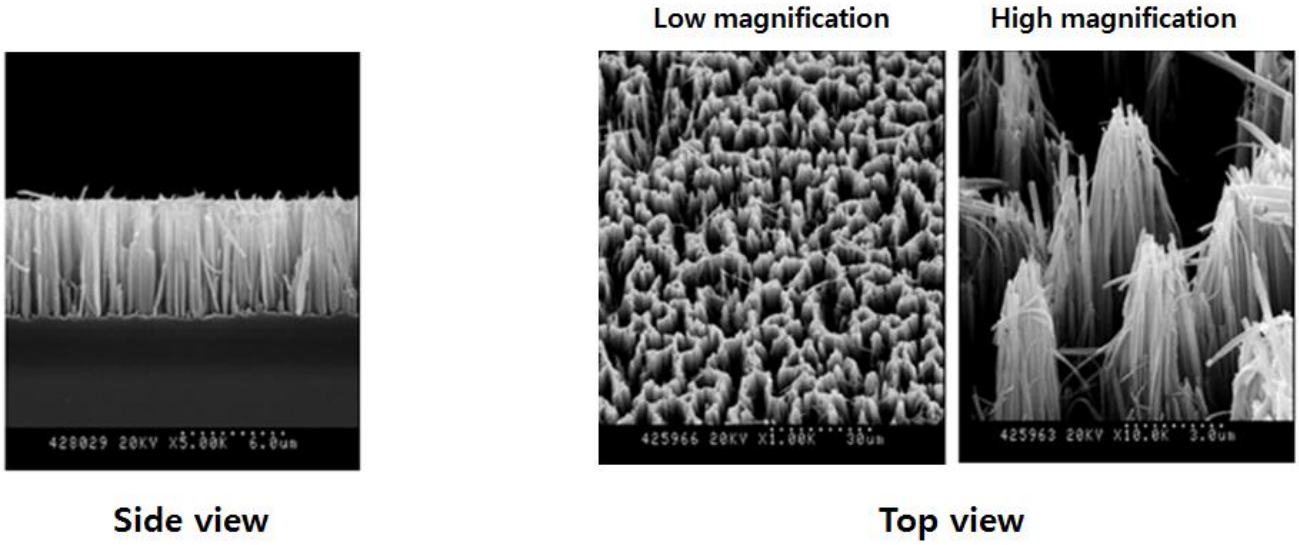

Figure S1. SEM images of vertically-aligned SiNWs.

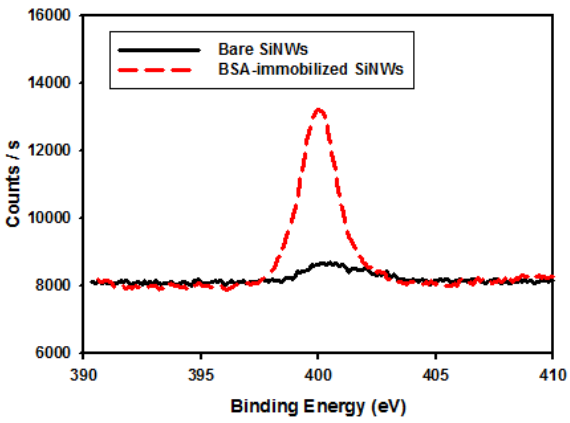

(a)

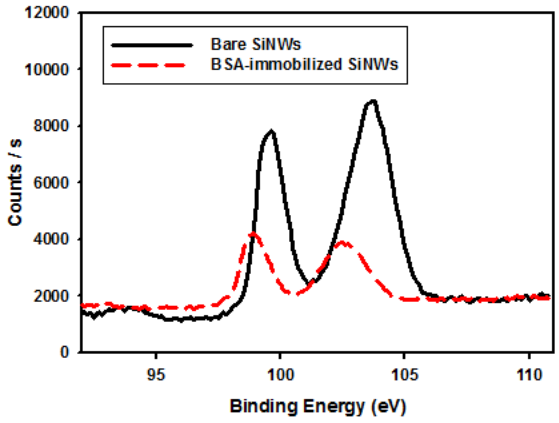

(b)

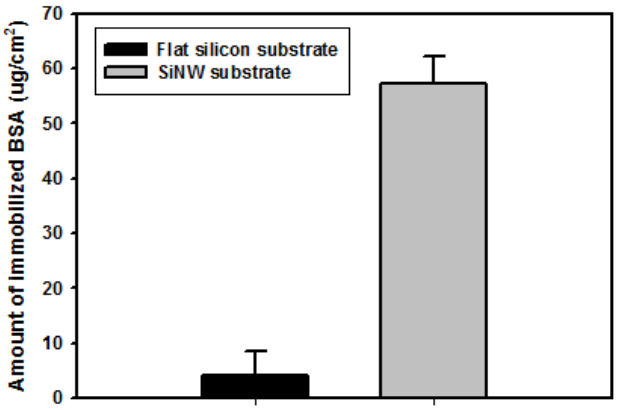

(c)

Figure S2. Protein immobilization onto SiNWs. XPS spectra of (a) N 1s and (b) Si 2p spectra for protein-immobilized and bare SiNW substrates. (c) The amount of BSA immobilized on planar silicon and SiNW substrates.

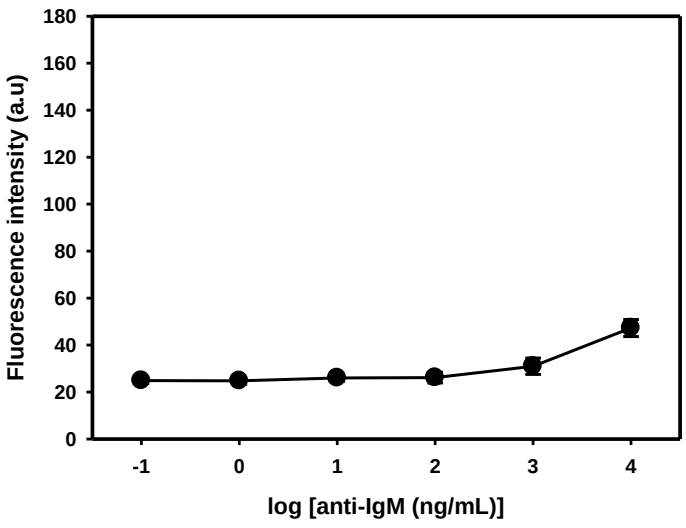

(a)

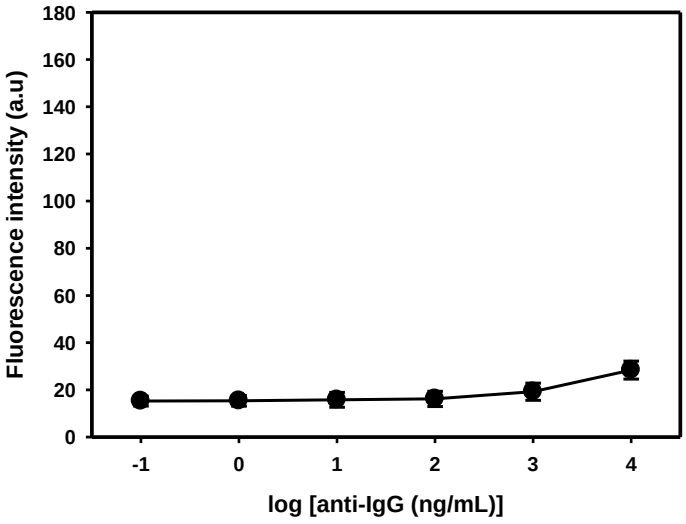

(b)

Figure S3. Specificity of SiNW-based immunoassay systems. (a) Change of fluorescence intensity when different concentrations of Cy3-anti IgM were reacted with IgG immobilized onto SiNWs. (b) Change of fluorescence intensity when different concentrations of FITC- anti IgG were reacted with IgM immobilized onto SiNWs. (Scales of x- and y-axis were set to same as Figure 3c and 3d for the comparison between specific and non-specific binding)

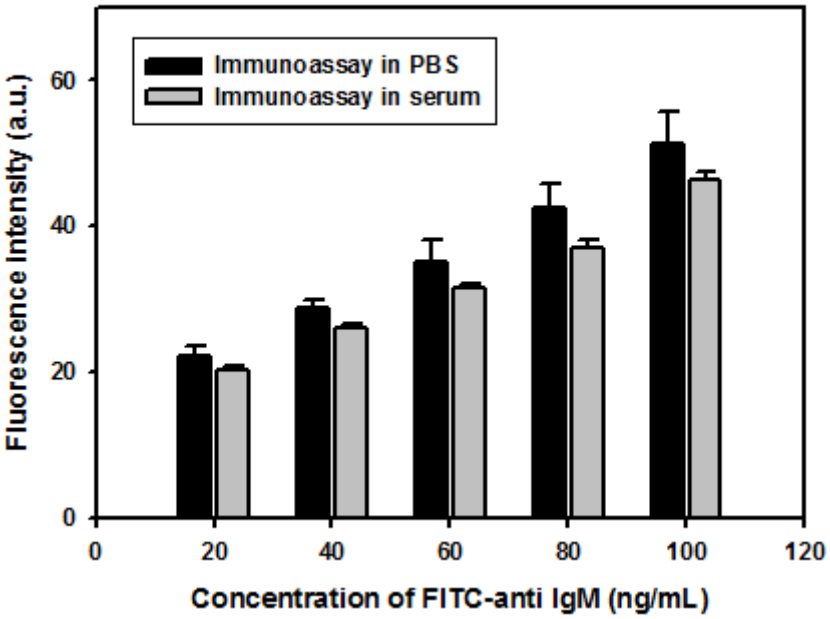

Figure S4. Comparison of detection performance between immunoassay in PBS and immunoassay in serum.

.